RSC Advances

PAPER

View Article Online
View Journal | View Issue

Cite this: *RSC Adv.*, 2024, **14**, 38697

Antiproliferative effects of resorcylic acid lactones from the Beibu Gulf coral-derived fungus *Curvularia lunata* GXIMD 02512 on prostate cancer cells†

Jiaxi Wang,‡[a] Humu Lu,‡[a] Wenxuan Fang,[ab] Miaoping Lin,[a] Yuyao Feng,[a] Xin Qi,[a] Chenghai Gao,[a] Yonghong Liu,[a] Xueni Wang*[b] and Xiaowei Luo *[a]

Received 31st August 2024
Accepted 24th November 2024

DOI: 10.1039/d4ra06292b

rsc.li/rsc-advances

Four novel resorcylic acid lactones (RALs), curvulomycins A–D (**1–4**), and six known congeners were isolated from the Beibu Gulf coral-derived fungus *Curvularia lunata* GXIMD 02512. Their structures including absolute configurations were established by extensive spectroscopic analyses along with experimental and calculated ECD spectra. Structurally, compound **3** harbors a unique γ-pyrone moiety rarely found in the natural RAL family. Notably, curvulomycin D (**4**) represents the first reported compound of the rare 8-membered RAL derivatives. Compounds **1** and **5** exhibited significant antiproliferative potency against two prostate cancer cell lines, with IC_{50} values of 9.70 ± 0.77 μM and 7.64 ± 0.46 μM for PC-3 cells and 5.96 ± 0.43 μM and 3.15 ± 0.27 μM for 22Rv1 cells, respectively. Moreover, compound **1** inhibited clonal cell colonies in a dose-dependent manner, blocked the S and G2 phases in the PC-3 cell cycle and the G1 phase in the 22Rv1 cell cycle, which further induced apoptosis in both PC-3 and 22Rv1 cells, indicating its potential as a promising lead compound for anti-prostate cancer therapy.

1. Introduction

Global cancer statistics for 2022 revealed nearly 20 million new cancer cases and close to 10 million cancer-related deaths. Projections suggest that the number of new cases will rise to 35 million by 2050, posing huge economic as well as societal challenges worldwide in the coming decades.[1] Prostate cancer (PC) is the most commonly diagnosed cancer in men, predominantly in regions with a high human development index. It remains the second most common malignancy and was the fifth leading cause of cancer-related deaths among men in 2022.[1,2] Patients with localized PC may progress to an advanced and lethal stage known as metastatic castration-resistant PC (CRPC) after undergoing standard therapeutic regimens. These treatments often result in poor outcomes owing to the lack of effective therapies.[3] Although current first-line therapies, such as AR antagonist enzalutamide and the androgen synthesis inhibitor abiraterone have shown initial improvement in the disease outcomes in some patients, *de novo* and acquired resistance continue to hinder the curable medications of CRPC.[4] Therefore, there is an urgent need for innovative molecular drugs with novel structures and more efficient and/or less toxic properties.

Natural products have consistently played a pivotal role in pharmaceutical research, exerting profound impacts on the treatment of human diseases, especially cancers.[5,6] Structurally complex compounds from traditional Chinese medicine as well as marine organisms have been recently evidenced as potential sources of new drugs against PC.[7,8] Notably, DD1, a daphnane diterpenoid isolated from *Daphne genkwa*, was identified as a highly potent importin-β1 inhibitor for the treatment of CRPC,[4] which was further optimized to an improved analog DD1-Br with better tolerability and oral bioavailability for overcoming drug resistance in advanced CRPC.[9] Elaiophylin, an antibiotic derived from marine *Streptomyces*, was found as a novel RORγ antagonist targeting CRPC, which strongly suppressed tumor growth in both cell line-based and patient-derived PC xenograft models.[10]

Resorcylic acid lactones (RALs) are fungal polyketides that consist of a β-resorcylic acid residue (2,4-dihydroxybenzoic acid) embedded in a macrolactone ring. The structural diversity of

[a]*Guangxi Key Laboratory of Marine Drugs, University Engineering Research Center of High-efficient Utilization of Marine Traditional Chinese Medicine Resources, Guangxi Institute of Marine Drugs, Guangxi University of Chinese Medicine, Nanning 530200, China. E-mail: luoxiaowei1991@126.com*

[b]*Guangxi Zhuang Yao Medicine Center of Engineering and Technology, Guangxi University of Chinese Medicine, Nanning 530200, China. E-mail: wangxueni@gxtcmu.edu.cn*

† Electronic supplementary information (ESI) available: ECD calculations, HRESIMS, 1D and 2D NMR, and UV spectra of compounds **1–4**. See DOI: https://doi.org/10.1039/d4ra06292b

‡ J. Wang and H. Lu contributed equally to this work.

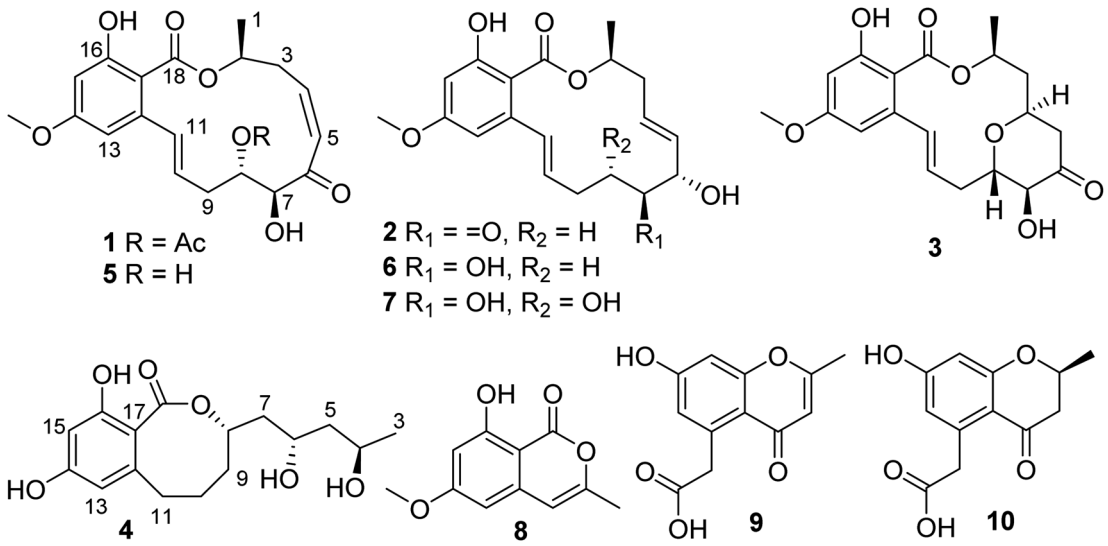

Fig. 1 Chemical structures of compounds **1**–**10**.

RALs is mainly due to the size as well as extensive modification of the macrolactone ring. Over 200 RALs have been reported from different genera of fungi hitherto, including *Aigialus*, *Curvularia*, *Lasiodiplodia*, *Penicillium*, *Pochonia*, and *Monocillium*, which were found to have diverse biological activities, including anticancer, antimicrobial, antimalarial, heat shock protein 90 (Hsp90) inhibitory, and protein tyrosine kinase inhibitory activities, eliciting considerable interest from communities of chemistry and pharmacology.[11,12] In the course of our continuous search for novel bioactive natural products from marine microorganisms, a series of anticancer compounds has been recently obtained, including ascochlorins,[13–16] piericidins,[17–19] epipolythiodioxopiperazines,[20] and azaphilones.[21] In this study, four new RALs and six known related congeners were obtained from the Beibu Gulf coral-derived fungus *Curvularia lunata* GXIMD 02512 by HPLC-DAD-guided isolation (Fig. 1). Herein, the isolation, structural elucidation, and anti-PC activities of these RALs along with their congeners are described in detail.

2. Results and discussion

Compound **1** was isolated as a white powder. The molecular formula was determined as $C_{21}H_{24}O_8$ by the HR-ESIMS peak at *m*/*z* of 427.1367 $[M + Na]^+$ (calcd for $C_{21}H_{24}O_8Na^+$, 427.1363), indicating 10 degrees of unsaturation (DOU). Its UV spectrum displayed UV absorption bands at 231, 270, and 309 nm, suggesting the presence of benzoic acid functionality in the structure. The ^{1}H NMR data (Table 1) in conjunction with HSQC data showed the presence of two methyls, H_3-1 (δ_H 1.38, d, J = 6.5 Hz) and H_3-2′ (δ_H 2.06, s), one methoxy group, H_3-19 (δ_H 3.75, s), two methylenes, H_2-3 (δ_H 2.64, m; 3.27, m) and H_2-9 (δ_H 2.19, m), three methines, H-2 (δ_H 5.22, m), H-7 (δ_H 4.52, dd, J = 5.0, 1.5 Hz), and H-8 (δ_H 5.03, m), and six aromatic/olefinic protons, H-4 (δ_H 6.32, td, J = 11.5, 3.0 Hz), H-5 (δ_H 6.49, dd, J = 11.5, 2.0 Hz), H-10 (δ_H 6.02, ddd, J = 16.0, 9.0, 5.5 Hz), H-11 (δ_H 6.76, d, J = 16.0 Hz), H-13 (δ_H 6.39, d, J = 2.5 Hz), and H-15 (6.40, d, J = 2.5 Hz). Apart from the above-mentioned proton-containing groups, there were seven quaternary carbons (δ_C 104.9, 141.8, 163.3, 163.4, 170.2, 170.4, and 199.2) in the ^{13}C NMR data of **1**. The spectroscopic features illustrated that **1** was a RAL derivative, which closely resembled those of co-isolated LL-Z1640-2 (**5**).[22] The main difference was the presence of an additional acetyl group ($\delta_{H/C}$ 2.06/21.1, CH_3-2′; δ_C 170.4, C-1′) at C-8 in **1** instead of a hydroxy group in **5**, which was confirmed by the HMBC correlations (Fig. 2) from H-8 and H_3-2′ to C-1′, along with the molecular formula. Further analysis of the HSQC, COSY, and HMBC data allowed the explicit assignment of all NMR resonances of **1**.

The relative configurations of **1** were determined by proton coupling constants and NOESY correlations. The large coupling constant between H-10 and H-11 (J = 15.5 Hz) along with the NOESY correlations (Fig. 2) of H-11/H_2-9 and H-10/H-13 revealed the *E* configuration of the Δ^{10} double bond. However, the *Z* configuration of the Δ^4 double bond in **1** was assigned by the small coupling constant ($J_{H\text{-}4/H\text{-}5}$ = 11.5 Hz), combined with the absent NOESY correlation of H-5/H_2-3. From a biosynthetic point of view, the absolute configurations of (2*S*, 7*S*, 8*S*) in **1** should be the same as those of **5**. This deduction was further ascertained by the shared nearly identical experimental ECD curves (Fig. 3) as well as the well matched calculated and experimental ECD curves of **1**, which showed shared positive Cotton Effect at about 230 nm and negative Cotton Effect at about 270 nm. Thus, the gross structure of **1** was resolved as shown in Fig. 1 and was given the trivial name curvulomycin A.

Curvulomycin B (**2**) was obtained as a white powder with the molecular formula $C_{19}H_{22}O_6$, as assigned by the HR-ESIMS data (9 DOU). Interpretation of the spectroscopic characteristics (Table 1) of **2** was also indicative of an RAL-like structure, which showed great similarity to that of co-isolated deoxyaigialomycin C (**6**).[22] The major difference was the presence of a carbonyl group (δ_C 210.2, C-7) in **2** instead of a hydroxy-methine one in **6**,

Table 1 ^{1}H NMR (500 MHz) and ^{13}C NMR (125 MHz) data of compounds **1–4**[a]

	1[b]		**2**[c]		**3**[c]		**4**[c]	
Pos	δ_C, type	δ_H (J in Hz)	δ_C, type	δ_H (J in Hz)	δ_C, type	δ_H (J in Hz)	δ_C, type	δ_H (J in Hz)
1	20.1, CH_3	1.38, d (6.5)	18.9, CH_3	1.42, d (6.5)	21.9, CH_3	1.40, d (6.5)		
2	73.7, CH	5.22, m	72.7, CH	5.52, m	73.7, CH	5.20, m		
3	36.3, CH_2	2.64, m; 3.27, m	38.3, CH_2	2.50, m	38.2, CH_2	1.66, dq (16.0, 1.5) 2.15, ddd (16.0, 11.0, 7.5)	24.2, CH_3	1.17, d (6.0)
4	145.4, CH	6.32, td (11.5, 3.0)	131.6, CH	6.28, ddd (15.5, 9.0, 6.0)	74.4, CH	4.60, m	65.5, CH	3.94, m
5	126.0, CH	6.49, dd (11.5, 2.0)	133.3, CH	5.43, dd, (15.5, 8.0)	47.5, CH_2	2.86, dd (15.0, 6.0) 2.41, dd (15.0, 5.0)	46.3, CH_2	1.45, t (6.0)
6	199.2, C		80.1, CH	4.81, d (8.0)	209.1, C		66.2, CH	3.92, m
7	78.3, CH	4.52, dd (5.0, 1.5)	210.2, C		77.1, CH	4.18, d (9.5)	45.7, CH_2	1.93, dt (14.0, 7.0) 1.63, dt (14.0, 6.0)
8	74.8, CH	5.03, m	35.7, CH_2	2.61, ddd (18.0, 6.5, 3.0) 3.25, ddd (18.0, 11.0, 3.0)	78.8, CH	3.91, td (9.5, 3.0)	80.4, CH	4.52, dd (16.0, 7.0)
9	33.0, CH_2	2.19, m	25.3, CH_2	2.39, m; 2.72, m	34.4, CH_2	2.40, overlapped 2.64, ddd (14.5, 9.0, 3.5)	35.3, CH_2	1.91, m; 1.79, m
10	130.9, CH	6.02, ddd (16.0, 9.0, 5.5)	132.2, CH	6.16, dt (16.0, 4.5)	127.4, CH	5.83, dt (16.0, 6.5)	28.0, CH_2	2.08, m; 1.56, m
11	131.5, CH	6.76, d (16.0)	129.7, CH	6.70, dt (16.0, 1.5)	136.5, CH	7.09, d (16.0)	34.2, CH_2	2.75, dd (13.5, 7.5) 2.58, t (13.5)
12	141.8, C		143.0, C		144.9, C		145.5, C	
13	106.4, CH	6.39, d (2.5)	106.9, CH	6.49, d (2.5)	108.0, CH	6.33, d (2.5)	109.4, CH	6.20, d (2.5)
14	163.4, C		165.0, C		165.3, C		162.8, C	
15	100.3, CH	6.40, d (2.5)	100.8, CH	6.28, d (2.5)	100.5, CH	6.35, d (2.5)	102.1, CH	6.23, d (2.5)
16	163.3, C		164.7, C		164.7, C		159.3, C	
17	104.9, C		106.8, C		106.9, C		110.7, C	
18	170.2, C		171.9, C		172.1, C		173.5, C	
19	55.5, CH_3	3.77, s	55.9, CH_3	3.79, s	55.9, CH_3	3.80, s		
1′	170.4, C							
2′	21.1, CH_3	2.06, s						

[a] For **1**, δ_H 5.41, d (5.0), 7-OH; 11.71, s, 16-OH. [b] In DMSO-d_6. [c] In CD_3OD.

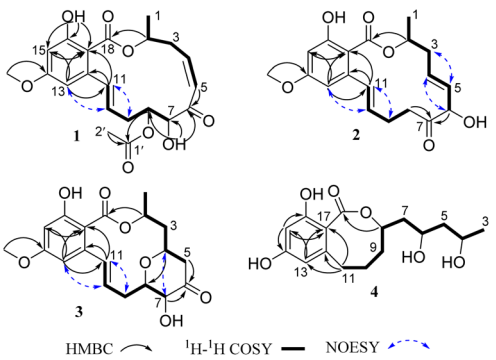

Fig. 2 Key HMBC, ^{1}H–^{1}H COSY, and NOESY correlations of compounds **1–4**.

which was confirmed by the HMBC correlations (Fig. 2) of C-7/H-6 (δ_H 4.81) and H_2-8 (δ_H 3.25, 2.61). Both Δ^4 and Δ^{10} double bonds were determined as *E* configuration based on the NOESY correlations and large proton coupling constants of $J_{H\text{-}4/H\text{-}5}$ (15.5 Hz) and $J_{H\text{-}10/H\text{-}11}$ (16.0 Hz).

As in the same case of **1**, the stereogenic carbon at C-2 in these obtained 14-membered RALs (**1–3** and **5–7**) was assigned as *S*-configuration on the basis of the shared biosynthetic origin. Thus, two possible diastereoisomers of **2** were further subjected to ECD calculations at the B3LYP/6-31+G (d, p) level by time-dependent density functional theory (TDDFT).[13] The calculated ECD curve (Fig. 3) of (2*S*, 6*S*)-**2** coincided well with the experimental one, suggesting (2*S*, 6*S*)-configuration of **2**.

Curvulomycin C (**3**) was isolated as a white powder with the molecular formula $C_{17}H_{20}O_4$ (6 DOU), as determined by the HR-ESIMS ion peak. The ^{1}H NMR data (Table 1) underscored the presence of one methyl, H_3-1 (δ_H 1.40, d, J = 6.5 Hz), one methoxy group, H_3-19 (δ_H 3.80, s), three methylenes, H_2-3 (δ_H 1.66, dq, J = 16.0, 1.5 Hz; 2.15, ddd, J = 16.0, 11.0, 1.5 Hz), H_2-5 (δ_H 2.41, dd, J = 15.0, 5.0 Hz; 2.86, dd, J = 15.0, 6.0 Hz), and H_2-9 (δ_H 2.40, overlapped; 2.64, ddd, J = 14.5, 9.0, 3.5 Hz), four oxygenated methines, H-2 (δ_H 5.20, m), H-4 (δ_H 4.60, m), H-7 (δ_H 4.18, d, J = 9.5 Hz), and H-8 (δ_H 3.91, td, J = 9.5, 3.0 Hz), and four aromatic/olefinic protons, H-10 (δ_H 5.83, dt, J = 16.0, 6.5 Hz), H-11 (δ_H 7.09, d, J = 16.0 Hz), H-13 (δ_H 6.33, d, J = 2.5 Hz), and H-15 (6.35, d, J = 2.5 Hz). Aside from the above 13 corresponding hydrogen-bearing carbons, six remaining quaternary carbons in the ^{13}C NMR data were attributed to two carbonyls (δ_C 172.1, 209.1) and four olefinics (δ_C 106.9, 144.9; two oxygenated ones, 164.7, 165.3). The above spectral data of **3** also revealed a 14-membered RAL analogue structurally related to (7′*E*)-6′-oxo-zeaenol,[22] except for the observation of oxygenated methine (CH-4) in **3**. Meanwhile, the aforementioned functionalities accounted for 8 out of 9 DOU, indicative of an additional ring in **3**. The key HMBC correlation of H-4/C-8 allowed the establishment of a γ-pyrone ring by an ether bridge. Further analysis of

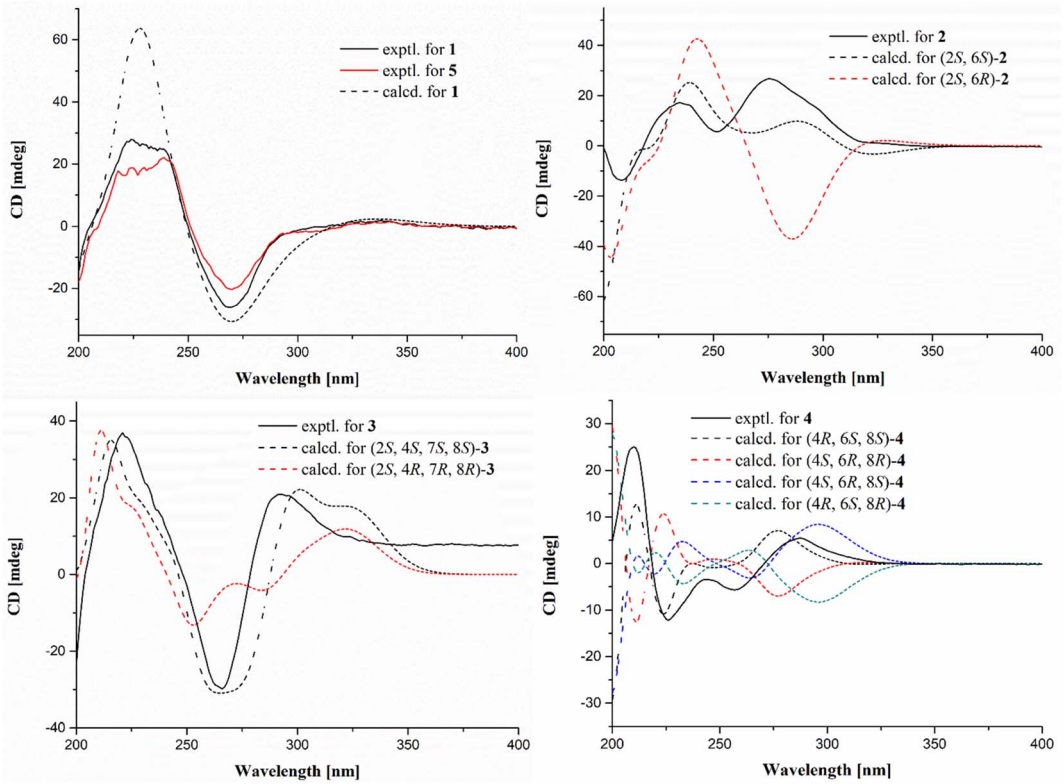

Fig. 3 Experimental and/or calculated ECD spectra of **1**–**5**.

the HSQC, COSY, and HMBC data confidently supported the NMR resonances of **3**. However, compound **3** was found as a synthetic RAL derivative from (5*Z*)-7-oxozeaenol,[23] which is relatively uncommon in the natural RAL family.

Similar to the case of **1** and **2**, the Δ^{10} double bond in **3** was also assigned the *E* configuration based on the NOESY correlations (Fig. 2) in association with a large proton coupling constant of 16.0 Hz. Moreover, the NOESY correlation of H-4/H-7 suggested that H-4 and H-7 were located on the same face of the γ-pyrone ring. Meanwhile, the absent NOESY correlation of H-4/H-8 tentatively revealed H-4 and H-8 were in the opposite side. This deduction was further confirmed by the anti-facial relationship of H-7/H-8, as deduced by the large proton coupling constant of 9.5 Hz in **3** (synthetic one: 9.6 Hz).[23] Further comparison between the experimental and calculated ECD spectra of **3** permitted the (2*S*,4*S*,7*S*,8*S*)-configuration of **3**.

Curvulomycin D (**4**) was obtained as a colorless oil with the molecular formula $C_{16}H_{22}O_6$ (6 DOU), as determined by HR-ESIMS data. The ^{1}H NMR data (Table 1) combined with HSQC data showed the signals indicative of one methyl, H_3-3 (δ_H 1.17, d, J = 6.0 Hz), five methylenes, H_2-5 (δ_H 1.45, d, J = 6.0 Hz), H_2-7 (δ_H 1.93, dt, J = 14.0, 7.0 Hz; 1.63, dt, J = 14.0, 6.0 Hz), H_2-9 (δ_H 1.91, m; 1.79, m), H_2-10 (δ_H 2.08, m; 1.56, m), and H_2-11 (δ_H 2.75, dd, J = 13.5, 7.5 Hz; 2.58, t, J = 13.5 Hz), three oxygenated methines, H-4 (δ_H 3.94, m), H-6 (δ_H 3.92, m), and H-8 (δ_H 4.52, dd, J = 16.0, 7.0 Hz), two aromatic protons, H-13 (δ_H 6.20, d, J = 2.5 Hz) and H-15 (δ_H 6.23, d, J = 2.5 Hz). Besides the 11 corresponding hydrogen-bearing carbons, five carbons remained in the ^{13}C NMR data, including one carbonyl (δ_C 173.5) and four aromatics (δ_C 110.7, 145.5; two oxygenated ones, 159.3, 162.8). The aforementioned NMR characteristics of **4** suggested the presence of a β-resorcylic acid ring (5 DOU) and a branched C_9 aliphatic chain with a 4,6,8-triol unit, which were confirmed by the HMBC correlations of H-13/C-15, C-17 and H-15/C-14, C-16, C-17 as well as sequential ^{1}H–^{1}H COSY correlations of H_3-3/H-4/H_2-5/H-6/H_2-7/H-8/H_2-9/H_2-10/H_2-11. Another ring was required to fulfill the remaining one DOU. Notably, the HMBC correlation of H-8/C-18 and H_2-11/C-12, C-13, C-17 allowed the establishment of a rare 8-membered lactone ring tethered to the β-resorcylic acid core. The relative configuration of the 4-OH/6-OH cluster was deduced as an anti-relationship by well-known Kishi's Universal NMR Database for the 1,3-diol moiety (Fig. 4).[24]

Many initial attempts exemplified by the modified Mosher's method applied to establish the absolute configurations of **4** turned failed, meanwhile more exhaustive efforts were hampered by the limited obtained quantity. With this

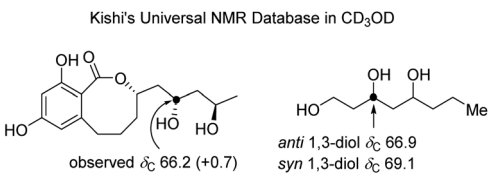

Fig. 4 Kishi's NMR data set for the elucidation of the relative configuration of the 1,3-diol moiety in compound **4**. $\Delta\delta_C$ value between **4** and the model system is shown in brackets.

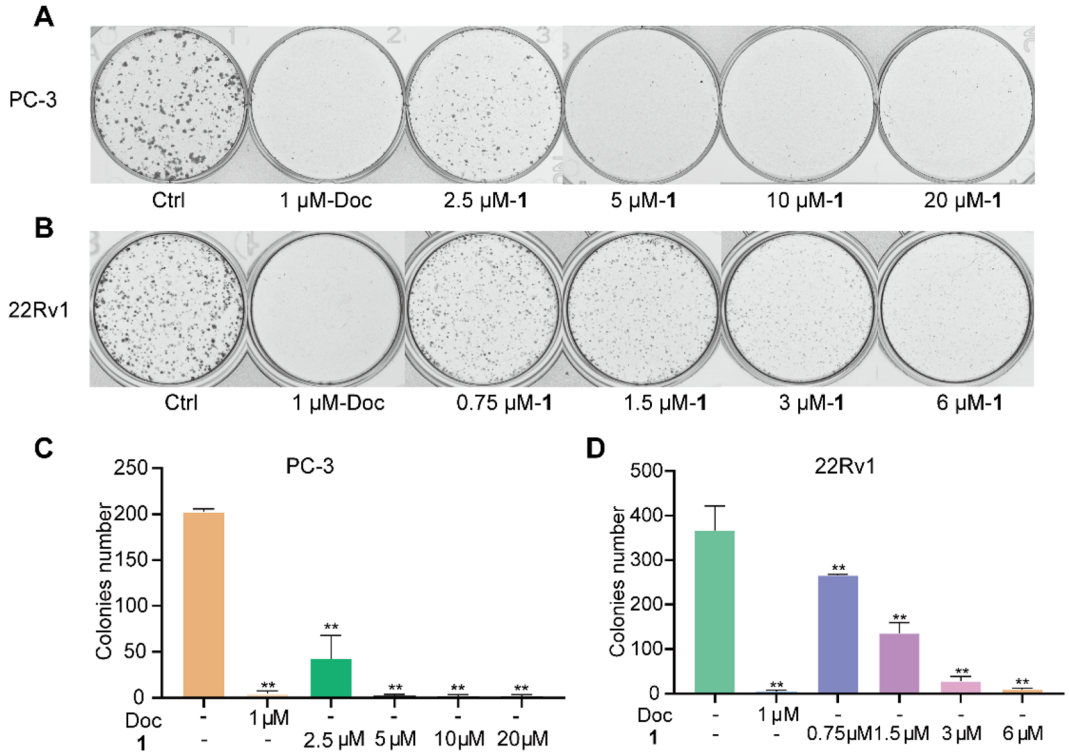

Fig. 5 Compound **1** inhibited the proliferation and clone formation of PC-3 (A and C) and 22Rv1 (B and D) cells. Each experiment was repeated at least three times independently. *P < 0.05, **P < 0.01 *vs.* Ctrl.

information in mind, four remaining possible stereoisomers of **4** were also alternatively subjected to ECD calculations. The calculated ECD spectrum of (11*S*,13*S*,15*R*)-**4** showed good agreement with the experimental one, indicating (11*S*,13*S*,15*R*)-configuration in **4** (Fig. 3). To our knowledge, curvulomycin D (**4**) is obtained as the first case of 8-membered RAL derivatives.

Meanwhile, the known compounds were identified by comparing their physicochemical and spectroscopic data with the literature values, which were LL-Z1640-2 (**5**),[22] deoxyaigialomycin C (**6**),[22] zeaenol (**7**),[22] 8-hydroxy-6-methoxy-3-methylisocoumarin (**8**),[25] 2-methyl-5-carboxymethyl-7-hydroxychromone (**9**),[26] and 2-methyl-5-carboxymethyl-7-hydroxychromanone (**10**).[26]

The cytotoxicity of compounds **1**–**10** toward two human PC cell lines, namely, 22Rv1 and PC-3, was tested using the MTT assay.[13,16,21] Amongst them, compounds **1** and **5** exhibited significant inhibitory activity with IC_{50} values of 9.70 ± 0.77 μM and 7.64 ± 0.46 μM for PC-3, and 5.96 ± 0.43 μM and 3.15 ± 0.27 for 22Rv1, respectively, which revealed that the acetyl group at C-8 in **1** would slightly decrease the inhibitory activity against the two PC cell lines. Moreover, compounds **1** and **5** were also tested in two normal PC cell lines, namely, WPMY-1 and RWPE-1, which also displayed cytotoxicities with IC_{50} values of 6.91 ± 0.12 μM and 5.74 ± 0.52 μM for WPMY-1, and 3.01 ± 0.09 μM and 3.18 ± 0.11 μM for RWPE-1, respectively.

We further examined the effects of the new compound **1** on the proliferation of two PC cell lines using a plate cloning assay. The experimental results showed that PC cells in the control group proliferated normally and formed dense clonal cell colonies. However, all PC cells in the docetaxel group were induced to undergo apoptosis and could not form obvious clonal cell colonies. Meanwhile, compound **1** showed significant inhibition of the PC clonal cell colonies in a dose-dependent manner (Fig. 5).

Confirming that compound **1** inhibited the proliferation of PC cells, we further examined its effect on the cell cycle and cell apoptosis by flow cytometry. PC-3 and 22Rv1 cells were treated with different concentrations of **1** (5 μM, 10 μM, and 20 μM) and docetaxel (1 μM) for 48 h. The results showed that the proportion of docetaxel-treated PC-3 and 22Rv1 cells in the G2/M phase was significantly higher than those of the control group, which verified that docetaxel blocked the cell cycle of both PC-3 and 22Rv1 cells at the G2/M phase. When PC-3 cells were treated with different concentrations of **1**, the percentage of cells in the G1 phase gradually decreased with increasing concentration, while the percentage of cells in the S and G2 phases increased (Fig. 6A and C). Meanwhile, the treatment of 22Rv1 cells with different concentrations of **1** resulted in a gradual increase in the percentage of cells in the G1 phase and a decrease in the percentage of cells in the S and G2 phases with increasing concentration (Fig. 6B and D). The above data suggested that **1** affected the cycle distribution of the two prostate cancer cell lines by blocking the cell cycle of PC-3 cells in the S and G2 phases, while it blocked the cell cycle of 22Rv1 cells in the G1 phase.

Meanwhile, PC-3 and 22Rv1 cells were also treated with different concentrations of **1** (5 μM, 10 μM, 20 μM, and/or 40

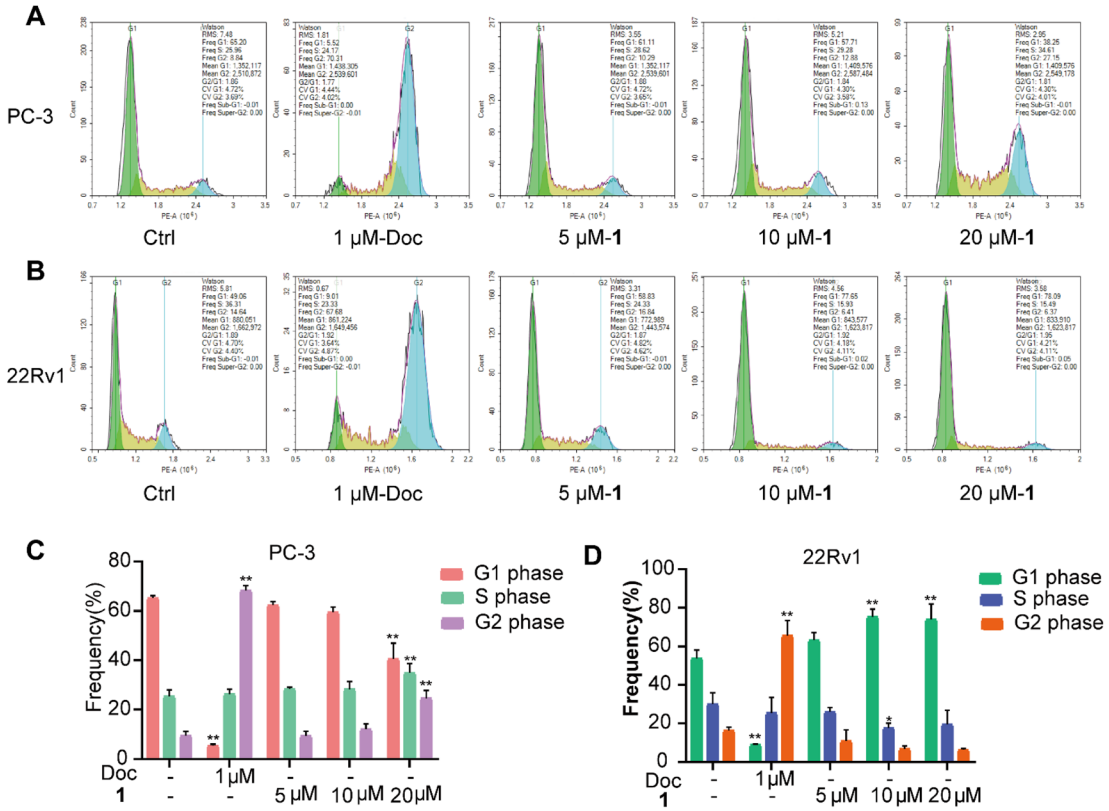

Fig. 6 Effect of **1** on the cell cycle of PC-3 (A and C) and 22Rv1 (B and D) cells *in vitro*. *$P < 0.05$, **$P < 0.01$ *vs.* Ctrl.

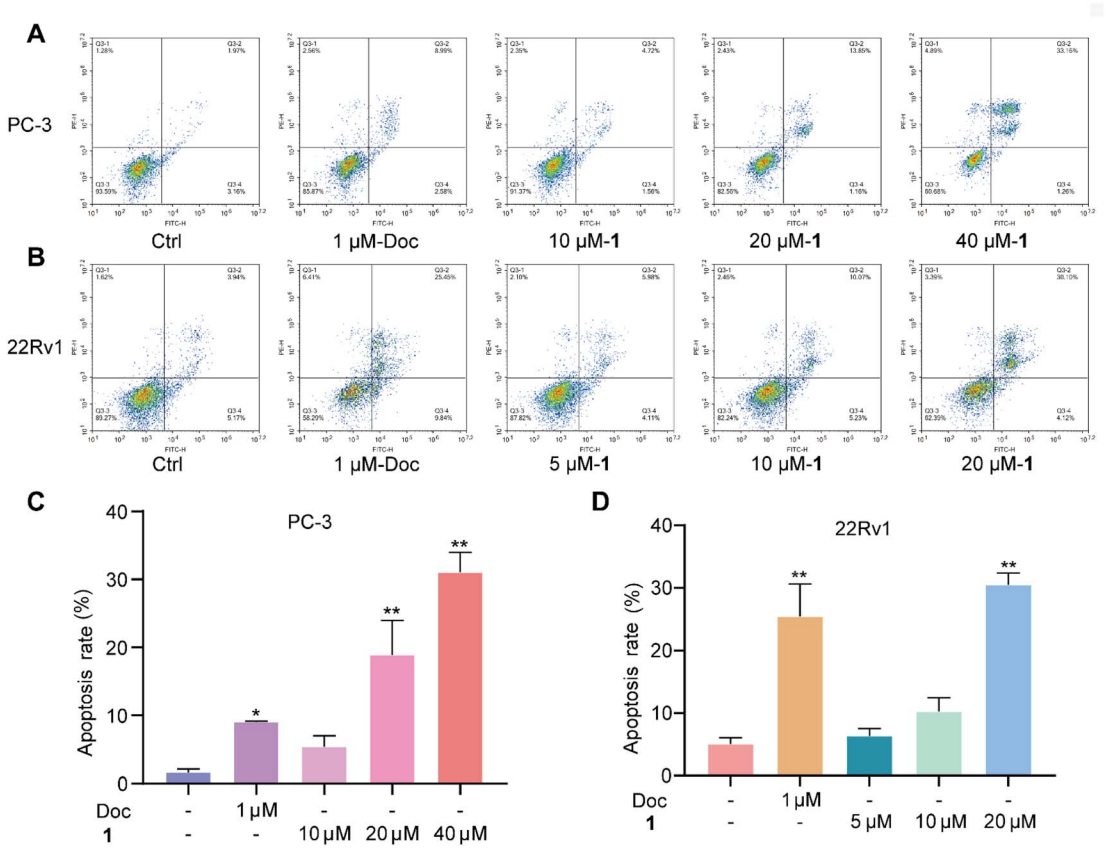

Fig. 7 Effect of **1** on the cell apoptosis of PC-3 (A and C) and 22Rv1 (B and D) cells *in vitro*. *$P < 0.05$, **$P < 0.01$ *vs.* Ctrl.

μM) and docetaxel (1 μM) for the evaluation of cell apoptosis. The total apoptotic cells (early and late apoptotic cells) induced by docetaxel rose by 11.6% for PC-3 cells and 35.3% for 22Rv1 cells at 1 μM (Fig. 7), respectively. Meanwhile, the total apoptotic cells induced by **1** rose by 15.0% for PC-3 cells (Fig. 7A and C) and 34.2% for 22Rv1 cells (Fig. 7B and D) at 20 μM, suggesting a promising anti-PC lead compound.

3. Experimental

3.1. General experimental procedures

The ECD spectra were measured on a JASCO J-1500 polarimeter (JASCO Corporation, Tokyo, Japan). The NMR spectra were obtained on a Bruker Avance spectrometer (Bruker BioSpin, Fällanden, Switzerland) operating at 500 MHz for ^{1}H NMR and 125 MHz for ^{13}C NMR, using TMS as an internal standard. HR-ESIMS spectra were collected on a Waters Xevo G2-S TOF mass spectrometer (Waters Corporation, Milford, MA, USA). TLC and column chromatography (CC) were performed on plates pre-coated with silica gel GF_{254} (10–40 μm) and over silica gel (200–300 mesh) (Qingdao Marine Chemical Factory, Qingdao, China), respectively. All solvents employed were of analytical grade (Shanghai Titan Scientific Co. Ltd, Shanghai, China). Semi-preparative high-performance liquid chromatography (Semi-prep HPLC) was performed on a Shimadzu SCL-10VAP (Shimadzu, Tokyo, Japan), equipped with an ODS column (YMC-pack ODS-A, YMC Co. Ltd, Kyoto, Japan, 10 × 250 mm, 5 μm, 2 mL min^{-1}). The artificial sea salt was a commercial product (Guangzhou Haili Aquarium Technology Company, Guangzhou, China).

3.2. Fungal material

The fungus GXIMD 02512 was isolated from the coral *Pocillopora damicornis* collected from the Weizhou Islands in Guangxi, China. It was taxonomically identified as *Curvularia lunata* GXIMD 02512 by sequence analysis of the internal spacer (ITS) region of the rDNA (GenBank accession no. PP535558). The voucher specimen was deposited at the Institute of Marine Drugs, Guangxi University of Chinese Medicine.

3.3. Fermentation, extraction, and isolation

The large-scale fermentation of *C. lunata* GXIMD 02512 was carried out in rice solid medium (120 g rice, 3.0 g artificial sea salt, 0.3 g corn steep liquor, and 150 mL H_2O) employing 1 L × 60 Erlenmeyer flasks at room temperature for 36 days. The rice fermentation products were extracted with ethyl acetate (EtOAc) and evaporated *in vacuo* to obtain the crude extract (73 g). The crude extract was divided by medium-pressure liquid chromatography using step gradient elution with petroleum ether/CH_2Cl_2/CH_3OH (petroleum ether/CH_2Cl_2, 100 : 0–0 : 100; CH_2Cl_2/methanol, 100 : 0–50 : 50, v/v). Nine fractions (Frs.1–9) were further combined and obtained according to TLC observations. Fr.8 was separated by reverse phase silica gel column chromatography, and 10 sub-fractions (Frs.8-1–8-10) were obtained by gradient elution (CH_3OH/H_2O, 10 : 90–100 : 0, v/v). Fr.8-5 was isolated by semi-prep HPLC (CH_3CN/H_2O, 50 : 50, 2 mL min^{-1}) to yield compounds **2** (t_R = 41 min, 9.1 mg) and **3** (t_R = 32 min, 4.5 mg). Fr.8-6 was purified by semi-prep HPLC (CH_3CN/H_2O, 58 : 42, 2 mL min^{-1}) to obtain compound **1** (t_R = 32 min, 2.8 mg).

Fr.9 was separated by reversed-phase silica gel column chromatography with gradient elution (CH_3OH/H_2O, 10 : 90–100 : 0, v/v) to provide 23 fractions. Fr.9-5 was isolated by semi-prep HPLC (CH_3CN/H_2O, 20 : 80, 2 mL min^{-1}) to afford compound **8** (t_R = 47 min, 11.7 mg) and three sub-fractions, namely, Frs.9-5-1–9-5-3 and Fr.9-5-1, were further purified by semi-prep HPLC (CH_3CN/H_2O, 20 : 80, 2 mL min^{-1}) to yield compounds **4** (t_R = 25 min, 4.1 mg) and **9** (t_R = 27.5 min, 5.2 mg). Fr.9-5-3 was purified using semi-prep HPLC (CH_3CN/H_2O, 30 : 70, 2 mL min^{-1}) to obtain compound **10** (t_R = 16 min 2.8 mg). Fr.9-12 was isolated by semi-prep HPLC (CH_3CN/H_2O, 48 : 52, 2 mL min^{-1}) to produce compounds **7** (t_R = 12.5 min, 28.8 mg), **5** (t_R = 21 min, 3.3 mg), and **6** (t_R = 23 min, 6.8 mg).

3.3.1 Curvulomycin A (1). White powder; $[\alpha]_D^{25}$ −12 (*c* 0.07, CH_3OH); UV (CH_3OH) λ_{max} (log ε) 231 (4.06), 270 (3.57), 309 (3.32) nm; ECD (0.25 mg mL^{-1}, CH_3OH) λ_{max} ($\Delta\varepsilon$) 229 (+26.5), 269 (−26.1) nm; ^{1}H NMR and ^{13}C NMR data, see Table 1; HR-ESIMS *m*/*z* 427.1367 $[M + Na]^+$(calcd for $C_{21}H_{24}O_8Na^+$ 427.1363).

3.3.2 Curvulomycin B (2). White powder; $[\alpha]_D^{25}$ +103 (*c* 0.6, CH_3OH); UV (CH_3OH) λ_{max} (log ε) 235 (4.21), 270 (3.83), 311 (3.50) nm; ECD (0.25 mg mL^{-1}, CH_3OH) λ_{max} ($\Delta\varepsilon$) 208 (−13.8), 235 (+17.1), 252 (+5.6), 276 (+26.7) nm; ^{1}H NMR and ^{13}C NMR data, see Table 1; HR-ESIMS *m*/*z* 369.1315 $[M + Na]^+$(calcd for $C_{19}H_{23}O_6^+$ 369.1309).

3.3.3 Curvulomycin C (3). White powder; $[\alpha]_D^{25}$ −15 (*c* 0.5, CH_3OH); UV (CH_3OH) λ_{max} (log ε) 229 (4.12), 265 (3.72), 303 (3.47) nm; ECD (0.25 mg mL^{-1}, CH_3OH) λ_{max} ($\Delta\varepsilon$) 221 (+11.7), 266 (−15.7), 293 (+5.1) nm; ^{1}H NMR and ^{13}C NMR data, see Table 1; HR-ESIMS *m*/*z* 361.1289 $[M - H]^-$(calcd for $C_{19}H_{21}O_7^-$ 361.1293).

3.3.4 Curvulomycin D (4). Colorless oil; $[\alpha]_D^{25}$ −26 (c 0.07, CH_3OH); UV (CH_3OH) λ_{max} (log ε) 200 (4.1205), 262 (3.38) nm; ECD (0.25 mg mL^{-1}, CH_3OH) λ_{max} ($\Delta\varepsilon$) 210 (+32.2), 226 (−15.6), 244 (−4.37), 287 (+7.07) nm; ^{1}H NMR and ^{13}C NMR data, see Table 1; HR-ESIMS *m*/*z* 333.1315 $[M + Na]^+$(calcd for $C_{16}H_{22}O_6Na^+$ 333.1309).

3.4. ECD calculations

Conformational analysis was subjected to Spartan'14 software (Wavefunction Inc., Irvine, CA, USA) using the Merck Molecular Force Field (MMFF), as previously described.[13,21] Low-energy conformers with a Boltzmann distribution over 1% were chosen for DFT/TD-DFT calculations by Gaussian 16 software (Gaussian, Wallingford, CT, USA) at the B3LYP/6-311+G (d, p)//B3LYP/6-31+G (d) level in methanol by adopting 50 excited states. The ECD spectra were generated by SpecDis 1.7 (University of Wurzburg, Wurzburg, Germany) using a half bandwidth of 0.2–0.3 eV, according to the Boltzmann-calculated contribution of each conformer after UV correction.

3.5. Cytotoxicity bioassay

Human prostate cancer PC-3 and 22Rv1 cells, along with human normal prostate RWPE-1 and WPMY-1 cells, were obtained from the Cell Bank/stem Cell Bank of the Chinese Academy of

Sciences. All cell lines were also cultured in the medium according to the recommendations of the Cell Bank/stem Cell Bank of the Chinese Academy of Sciences. Cells in logarithmic growth phase were inoculated into 96-well cell culture dishes with 5000 cells per well. After all cells were attached to the bottom of the plate, the cells were primarily treated with these obtained compounds with a screening concentration of 10 μM. Compounds **1** and **5** with inhibitions over 50% were further subjected to the gradient test by the MTT method,[16] which were 0.3125 μM, 0.625 μM, 1.25 μM, 2.5 μM, 5 μM, 10 μM, 20 μM, and 40 μM, while the control group was treated with dimethyl sulfoxide (DMSO, 0.1%, D8371, Solarbio). After the cells were treated by the compounds for 72 h, MTT solution (M8180, Solarbio) was added to the reaction with the cells for 4 h. Then, the OD values were detected by a multiwell plate reader (Synergy™ H1, Bio-Tek), and the IC_{50} values were fitted with GraphPad Prism 8.0. Docetaxel was used as the positive control with IC_{50} values of 0.12 μM and 0.030 μM for PC-3 and 22Rv1 cells, respectively.

3.6. Clone formation assay

PC-3 cells and 22Rv1 cells were inoculated into 6-well plates, and compound **1** was added to treat the cells after they were completely attached to the bottom of the wells. In PC-3 cells, the concentration gradient of **1** was 2.5 μM, 5 μM, 10 μM, and 20 μM. In 22Rv1 cells, the concentration gradient of **1** was 0.75 μM, 1.5 μM, 3 μM, and 6 μM. Docetaxel (S1148, Selleck, China) was added to the positive drug control at a concentration of 1 μM, and DMSO was added to the control at a concentration of 0.1% (v/v). After one week of compound treatment, the cells were given fresh medium and compound treatment again. Two weeks later, obvious clonal colonies of the cells were formed, then the cells were fixed with 4% cell tissue fixative (P1110, Solarbio), stained with crystal violet (G1063, Solarbio), and finally, the photographs of the clonal colonies of the cells were taken with a colony counter (GelCount™, Oxford-Optronix).

3.7. Cell cycle and apoptosis assays

Cells were inoculated into 6-well plates at a density of 2.0×10^5 per well for 48 h and then treated with either DMSO (0.1%, v/v), docetaxel (1 μM), or compound **1** (5, 10, and 20 μM) for 48 h, respectively. Cells were digested and collected with 0.25% trypsin solution and fixed with 75% ice ethanol overnight. Cells were then stained with FxCycle™ PI/RNase solution (F10797, Invitrogen) for 30 min and the cell cycle distribution was examined by flow cytometry (NovoCyte 2060R, ACEA Biosciences).

The cells were inoculated with 2.0×10^5 cells per well and cultured in 6-well plates for 48 h, which were then treated with **1**. PC-3 cells were treated with **1** at concentrations of 10, 20, and 40 μM, and 22Rv1 cells were treated with **1** at concentrations of 5, 10, and 20 μM. Docetaxel functioned as the positive control with a concentration of 1 μM. DMSO was added to the control group at a concentration of 0.1% (v/v). Then, the cells were cultured for 48 h and collected with 0.25% trypsin solution without EDTA (T1350, Solarbio), which were stained with propidium iodide and Annexin-V/FITC (BMS500FI-300, Invitrogen) according to the manufacturer's instructions. Cell apoptosis was detected and analyzed by flow cytometry (NovoCyte 2060R, ACEA Biosciences).

4. Conclusions

In summary, four new RALs and six known congeners were identified from the Beibu Gulf coral-derived fungus *Curvularia lunata* GXIMD 02512. To our knowledge, curvulomycin C (**3**) harboring a unique γ-pyrone ring is relatively uncommon in the natural RAL family. Notably, curvulomycin D (**4**) is obtained as the first case of rare 8-membered RAL derivatives. Curvulomycin A (**1**) and LL-Z1640-2 (**5**) exhibited significant antiproliferative activity against two prostate cancer cell lines with IC_{50} values of 9.70 ± 0.77 μM and 7.64 ± 0.46 μM for PC-3 cells, 5.96 ± 0.43 μM and 3.15 ± 0.27 μM for 22Rv1 cells, respectively. The acetyl group at C-8 in **1** would slightly decrease the inhibitory activity. Moreover, compound **1** inhibited clonal cell colonies in a dose-dependent manner, blocked S and G2 phases in the PC-3 cell cycle and the G1 phase in the 22Rv1 cell cycle, which further induced apoptosis in PC-3 and 22Rv1 cells. Collectively, our findings could expand the chemical and biological diversity of natural RALs and provide a promising anti-PC lead compound.

Data availability

The data supporting this article have been included as part of the ESI.†

Author contributions

Jiaxi Wang: data curation, investigation, methodology, writing – original draft. Humu Lu: data curation, methodology, funding acquisition. Wenxuan Fang: data curation, investigation. Miaoping Lin: data curation, formal analysis. Yuyao Feng: investigation, validation. Xin Qi: investigation, validation. Chenghai Gao: methodology, validation. Yonghong Liu: project administration. Xueni Wang: conceptualization, writing – review & editing. Xiaowei Luo: conceptualization, funding acquisition, project administration, resources, supervision, writing – review & editing.

Conflicts of interest

The authors declare that they have no known competing financial interests or personal relationships that could have appeared to influence the work reported in this paper.

Acknowledgements

This work was supported by Natural Science Foundation of Guangxi (2024GXNSFFA010004, 2024GXNSFBA010145), National Natural Science Foundation of China (U20A20101, 82260692), Guangxi Young and Middle-aged University Teachers' Scientific Research Ability Enhancement Project (2023KY0296), High-Level Talent Training Project Foundation

of Guangxi University of Chinese Medicine (GUCM) (No. 202407, 2022C038), Foundation of GUCM (2023QN004).

References

1 F. Bray, M. Laversanne, H. Sung, J. Ferlay, R. L. Siegel, I. Soerjomataram and A. Jemal, *Ca-Cancer J. Clin.*, 2024, **74**, 229–263, DOI: 10.3322/caac.21834.

2 R. J. Rebello, C. Oing, K. E. Knudsen, S. Loeb, D. C. Johnson, R. E. Reiter, S. Gillessen, T. V. D. Kwast and R. G. Bristow, *Nat. Rev. Dis. Primers.*, 2021, **7**, 9, DOI: 10.1038/s41572-020-00243-0.

3 J. J. Xie, H. He, W. N. Kong, Z. W. Li, Z. T. Gao, D. Q. Xie, L. Sun, X. F. Fan, X. Q. Jiang, Q. G. Zheng, G. Li, J. D. Zhu and G. Y. Zhu, *Nat. Chem. Biol.*, 2022, **18**, 1341–1350, DOI: 10.1038/s41589-022-01151-y.

4 J. L. Huang, X. L. Yan, W. Li, R. Z. Fan, S. Li, J. H. Chen, Z. H. Zhang, J. Sang, L. Gan, G. H. Tang, H. W. Chen, J. J. Wang and S. Yin, *J. Am. Chem. Soc.*, 2022, **144**, 17522–17532, DOI: 10.1021/jacs.2c06449.

5 Z. W. Luo, F. C. Yin, X. B. Wang and L. Y. Kong, *Chin. J. Nat. Med.*, 2024, **22**, 195–211, DOI: 10.1016/S1875-5364(24)60582-0.

6 D. J. Newman and G. M. Cragg, *J. Nat. Prod.*, 2020, **83**, 770–803, DOI: 10.1021/acs.jnatprod.9b01285.

7 F. M. Kong, C. R. Wang, J. Zhang, X. Q. Wang, B. X. Sun, X. Xiao, H. J. Zhang, Y. Q. Song and Y. J. Jia, *Chin. Herb. Med.*, 2023, **15**, 485–495, DOI: 10.1016/j.chmed.2023.05.003.

8 E. Montuori, C. A. C. Hyde, F. Crea, J. Golding and C. Lauritano, *Int. J. Mol. Sci.*, 2023, **24**, 1435, DOI: 10.3390/ijms24021435.

9 J. L. Huang, X. L. Yan, D. Huang, L. Gan, H. H. Gao, R. Z. Fan, S. Li, F. Y. Yuan, X. Y. Zhu, G. H. Tang, H. W. Chen and J. J. Wan, *Acta Pharm. Sin. B*, 2023, **13**, 4934–4944, DOI: 10.1016/j.apsb.2023.07.017.

10 J. W. Zheng, J. F. Wang, Q. Wang, H. Y. Zou, H. Wang, Z. H. Zhang, J. H. Chen, Q. Q. Wang, P. X. Wang, Y. S. Zhao, J. Lu, X. L. Zhang, S. T. Xiang, H. B. Wang, J. P. Lei, H. W. Chen, P. Q. Liu, Y. H. Liu, F. H. Han and J. J. Wang, *Acta Pharm. Sin. B*, 2020, **10**, 2313–2322, DOI: 10.1016/j.apsb.2020.07.001.

11 S. Kuttikrishnan, K. S. Prabhu, A. H. Al Sharie, Y. O. Al Zu'bi, F. Q. Alali, N. H. Oberlies, A. Ahmad, T. El-Elimat and S. Uddin, *Drug Discovery Today*, 2022, **27**, 547–557, DOI: 10.1016/j.drudis.2021.10.001.

12 W. F. Xu, N. N. Wu, Y. W. Wu, Y. X. Qi, M. Y. Wei, L. M. Pineda, M. G. Ng, C. Spadafora, J. Y. Zheng, L. Lu, C. Y. Wang, Y. C. Gu and C. L. Shao, *Mar. Life Sci. & Technol.*, 2022, **4**, 88–97, DOI: 10.1007/s42995-021-00103-0.

13 X. W. Luo, G. D. Cai, Y. F. Guo, C. H. Gao, W. F. Huang, Z. H. Zhang, H. M. Lu, K. Liu, J. H. Chen, X. F. Xiong, J. P. Lei, X. F. Zhou, J. J. Wang and Y. H. Liu, *J. Med. Chem.*, 2021, **64**, 13918–13932, DOI: 10.1021/acs.jmedchem.1c01402.

14 Z. H. Zhang, Y. D. Zhang and C. J. Yang, *Cell Biol. Int.*, 2021, **45**, 2380–2390, DOI: 10.1002/cbin.11674.

15 L. Guo, X. W. Luo, P. Yang, Y. T. Zhang, J. L. Huang, H. Wang, Y. F. Guo, W. F. Huang, Z. Q. Chen, S. S. Wang, J. J. Wang, J. P. Lei, S. T. Xiang and Y. H. Liu, *Front. Pharmacol.*, 2021, **12**, 723729, DOI: 10.3389/fphar.2021.723729.

16 X. Gan, X. W. Luo, J. Q. Chen, W. X. Fang, M. Y. Nie, H. M. Lu, Y. H. Liu and X. N. Wang, *Mol. Cell. Biochem.*, 2024, DOI: 10.1007/s11010-024-05026-9.

17 P. Yu, T. W. Gu, Y. Y. Rao, W. M. Liang, X. Zhang, H. G. Jiang, J. D. Lu, J. L. She, J. M. Guo, W. Yang, Y. H. Liu, Y. F. Tu, L. Tang and X. F. Zhou, *Acta Pharm. Sin. B*, 2024, **14**, 3232–3250, DOI: 10.1016/j.apsb.2024.03.005.

18 Z. Liang, Y. L. Chen, T. W. Gu, J. L. She, F. H. Dai, H. G. Jiang, Z. K. Zhan, K. L. Li, Y. H. Liu, X. F. Zhou and L. Tang, *J. Med. Chem.*, 2021, **64**, 9943–9959, DOI: 10.1021/acs.jmedchem.1c00175.

19 X. F. Zhou, Z. Liang, K. L. Li, W. Fang, Y. X. Tian, Y. X. Tian, X. W. Luo, Y. L. Chen, Z. K. Zhan, T. Zhang, S. R. Liao, S. W. Liu, Y. H. Liu, W. Fenical and L. Tang, *J. Med. Chem.*, 2019, **62**, 7058–7069, DOI: 10.1021/acs.jmedchem.9b00598.

20 M. P. Lin, Z. Z. Tang, J. X. Wang, H. M. Lu, C. W. Wang, Y. T. Zhang, X. M. Liu, Y. H. Liu and X. W. Luo, *J. Zhejiang Univ., Sci., B*, 2023, **24**, 275–280, DOI: 10.1631/jzus.B2200622.

21 X. W. Luo, X. P. Lin, H. M. Tao, J. F. Wang, J. Y. Li, B. Yang, X. F. Zhou and Y. H. Liu, *J. Nat. Prod.*, 2018, **81**, 934–941, DOI: 10.1021/acs.jnatprod.7b01053.

22 W. F. Xu, X. J. Xue, Y. X. Qi, N. N. Wu, C. Y. Wang and C. L. Shao, *Nat. Prod. Res.*, 2021, **35**, 490–493, DOI: 10.1080/14786419.2019.1633646.

23 L. Fakhouri, T. El-Elimat, D. P. Hurst, P. H. Reggio, C. J. Pearce, N. H. Oberlies and M. P. Croatt, *Bioorgan. Med. Chem.*, 2015, **23**, 6993–6999, DOI: 10.1016/j.bmc.2015.09.037.

24 Y. Kobayashi, C. H. Tan and Y. Kishi, *Helv. Chim. Acta*, 2000, **83**, 2562–2571, DOI: 10.1002/1522-2675(20000906)83:9<2562::AID-HLCA2562>3.0.CO;2-Z.

25 L. X. Feng, B. Y. Zhang, H. J. Zhu, L. Pan and F. Cao, *Chem. Nat. Compd.*, 2020, **56**, 974–976, DOI: 10.1007/s10600-020-03206-9.

26 Y. Kashiwada, G. Nonaka and I. Nishioka, *Chem. Pharm. Bull.*, 1984, **32**, 3493–3500, DOI: 10.1248/cpb.32.3493.